Title: Nurr1 orchestrates claustrum development and functionality

Authors: Kuo Yan[1], Andrew Newman[1], Pauline Lange[1], Susanne Mueller[2,3,4], Marco Foddis[2,3,4], Maron Mantwill[2,3,4], Carsten Finke[2,3,4], Stefan Paul Koch[2,3,4], Philipp Boehm-Sturm[2,3,4], Penghui Deng[1], Melissa Long[5], Victor Tarabykin[1,6]*

Affiliations:

[1] Institute of Cell Biology and Neurobiology, Charité-Universitätsmedizin Berlin, corporate member of Freie Universität Berlin and Humboldt-Universität zu Berlin, Germany;

[2] Charité 3^{R} – Replace | Reduce | Refine, Charité-Universitätsmedizin Berlin, corporate member of Freie Universität Berlin and Humboldt-Universität zu Berlin, Germany;

[3] Department of Experimental Neurology and Center for Stroke Research Berlin, Charité-Universitätsmedizin Berlin, corporate member of Freie Universität Berlin and Humboldt-Universität zu Berlin, Germany;

[4] Charité Core Facility Experimental MRIs, Charité-Universitätsmedizin Berlin, corporate member of Freie Universität Berlin and Humboldt-Universität zu Berlin, Germany;

[5]Animal Behavior Phenotyping Facility, Charité-Universitätsmedizin Berlin, corporate member of Freie Universität Berlin and Humboldt-Universität zu Berlin, Germany;

[6]Institute of Neurosciences, Laboratory of Genetics of Brain Development, Lobachevsky State University of Nizhny Novgorod, Nizhny Novgorod, Russia

*Corresponding authors. Email: victor.tarabykin@charite.de

Abstract

In spite of the lasting controversy on claustrum's roles in consciousness formation, claustrum is known the most widely interconnected tissue with almost all brain subareas to coordinate multiple cognitive behaviors. However, little is known about the molecular mechanisms underlying its development and behavioral control. Here we show that Nurr1 (Nr4a2) is the key factor orchestrating claustral morphogenesis, functional connectivity and thus behaviors. Nurr1 deficient claustral cells over-migrate into insular cortex, shaping claustrum into an

abnormal wing-like structure, and ectopically turn on insular cortical genetic program. Accordingly, functional connectivity associated with claustrum and relevant behaviors are dysregulated by Nurr1 deficiency. Additionally, Nurr1 regulates claustral neuron positioning by suppressing G-protein signaling.

Introduction

The claustrum (CLA), a sheet-like gray matter structure resident between striatum and insular cortex in mice, exists in most vertebrate species ranging from birds, reptiles, rodents to human[1-4.] Little attention has been paid to this thin structure since being identified 200 years ago until Crick and Koch proposed that CLA be the processing hub of sensory information from multiple cerebral sources to integrate coherent consciousness[5]. Though whether CLA is the core hardware of consciousness is still uncertain to date, it is indeed intensively interconnected to almost all global subareas[4, 6-8], empowering its involvement in diverse cognitive activities, including but not limited to stress responses, attention, salient sensation, sensorimotor cross-modal selection, sleep and pain perception[9-14]. The insights into nerve circuitry underlying these physiological functions are accumulating due to recent advancement of optogenetics[9, 15,16], very little, however, has been elucidated about the molecular mechanisms governing CLA development and cognitive behaviors yet.

Nurr1 (Nr4a2) is a transcription factor (TF) that contains a single zinc-finger DNA-binding domain. It is not only renowned to promote dopaminergic neurogenesis as well as dopamine production in substantia nigra[17, 18], but also the most frequently used marker for CLA glutamatergic neurons[1, 19, 20]. Nurr1 expression in CLA neurons is already onset as early as E13 and lasts throughout life in mice (*Allen brain atlas*), but its role in CLA remains largely unknown. Here we demonstrate novel evidence that Nurr1's transcription activity is indispensable to orchestrate claustral morphogenesis, cell identity specification, functional connectivity and CLA-regulated cognitive behaviors.

Results

Transcription activity of Nurr1 is necessary for claustrum morphogenesis

We initially wanted to characterize Nurr1's roles in cortical development, and thus generated Nurr1 conditionally deficient mice regulated by EmxCre (Nurr1$^{flox/flox}$;EmxCre$^{Cre/Wt}$, Nurr1 deficient mice throughout text unless otherwise noted), where the floxed exon 3 of Nurr1's transcript containing the start codon and DNA-binding domain was selectively depleted in cortical progenitors at ~E10 by Cre recombinase under the control of Emx1 promoter[21]. The genetic design of Nurr1$^{flox/flox}$ mouse model entitles a likelihood to trace Nurr1-expressing cells absent of its transcription regulatory activity in Cre-present brains in that a C-terminal (Cterm) truncated open reading frame of Nurr1 consistent with the original transcript under control of the same Nurr1 promoter might be still present while recombined[18]. To testify this, we procured antibodies to target N-terminal (Nterm) and Cterm portions of Nurr1 protein, as well as *in situ* hybridization (ISH) probes to target Nurr1 5'- and 3'-terminal transcripts (5'end and 3'end), respectively (Fig. 1A). While ISH by the 5'end probe verified Nurr1 expression disruption in mutant brains (Fig. S1A), Nurr1 3'end mRNA was still detectable in CLA, subplate (Sb), dorsal endopiriform nuclei (dEn), subiculum (Sb) and cortical plate (CP) (Fig. S1B), similar with Nurr1 expression in controls. Likewise, immunofluorescence (IF) using Nurr1 Nterm and Cterm antibodies confirmed the same results (Fig. S1C). Notably, the truncated Nurr1-Cterm polypeptide loses nuclear localization (Fig. S1C) due to depletion of nuclear localization signal peptide[22], indicating its inability to regulate transcription.

The general anatomy of Nurr1 deficient cortex are basically normal (Fig. S2A-B), consistent with previous reports[17, 18]. We then focused on the Nurr1-expressing structures and found that Sp appears basically normal in morphology by Nurr1 deficiency using ISH for Sp markers - CTGF and S100a10[23, 24] (Fig. S2C-D). ISH for Zbtb20, a hippocampal marker[25, 26], in developing and postnatal brains suggests that the formation of perisubicular complexes is also normal in Nurr1 deficient brains (Fig. S2E-F). Additionally, co-IF for Nurr1 and Zbtb20 depicts that Nurr1-positive (Nurr1+) Sb delineates borders to separate neocortical cingulate cortex from hippocampal distal CA1, which maintains comparable in control and mutant brains (Fig. S2G). In contrast, both IF and ISH data demonstrate that Nurr1 deficient CLA cells detach from Sp and invade into insular cortex (InC) in both sagittal and coronal views at P2 (Fig. 1B-C). To further confirm the dislocation of Nurr1 deficient CLA cells, we performed ISH for Cux2, another CLA cell marker[20], and found Cux2+ CLA cells become ectopically present in InC of Nurr1 deficient brains (Fig. 1D). Consequently, the CLA is reshaped from a crescent-like into a wing-like structure (Fig. S3A). We next asked if the

ectopic CLA cells in InC of Nurr1 deficient brains are due to over-production of Nurr1-expressing cells. We quantified Nurr1-Cterm+ cells in claustro-insular region and found its number in Nurr1 deficient brains is similar with that in controls (Fig. S3B). Furthermore, few cleaved-Caspase3+ cells were detected in the claustro-insular regions of control and mutant brains (Fig. S3C-D). Nurr1 thus does not play a role in CLA neuron productivity or survival.

We then questioned what happened to the original CLA territory when Nurr1 deficient cells move away. IF for Nurr1-Cterm and Tle4/Darpp32 delineates CLA cells from neighboring InC deeper layer (DL) neurons in control brains, depicting normal CLA cells are bilaterally restricted in an area between stratum and InC DL neurons. However, Nurr1 deficient CLA cells have largely bypassed InC DL cells since E17.5 (Fig. 1E). Intriguingly, Tle4/Darpp32-expressing DL cells, which avoid to inhabit in CLA in controls, are filled in the original CLA territory in Nurr1 deficient brains (Fig. 1E), an observation further strengthened by ISH for Fezf2 and Nfib (Fig. S4). It has been proposed Nurr1+ neurons can migrate radially and tangentially to CLA and neocortex[19], we next wanted to study the migration mode of Nurr1 deficient CLA cells. IF for Nurr1-Cterm and Nestin shows Nurr1-Cterm+ CLA cells in mutant brains constitutively migrate towards pia along Nestin+ radial glia scaffold throughout cortical neurogenesis (Fig. 1F), thus spoiling the laminated organization of claustro-insular tissues (Fig. 1G). Collectively, Nurr1 orchestrates multiple aspects of CLA morphogenesis, such as positioning and interaction with adjacent tissues, to make CLA such distinct cytoarchitecture.

Another key question is whether Nurr1 determines CLA cell positioning pre- or postmitotically. To answer this, we generated Nurr1$^{flox/flox}$;NexCre$^{Cre/Wt}$ mice, in which Nurr1 is selectively inactivated in cortical postmitotic compartment[27]. It turned out that Nurr1 NexCre mutant brains fully recapitulated the morphological phenotypes as in EmxCre mutant brains (Fig. S5A-B), suggesting Nurr1's role in postmitotic regulation.

Nurr1 controls claustral neuron specification postmitotically

We next desired to find out if Nurr1 also plays a role in CLA cell specification. To this end, we first performed ISH for several CLA marker genes, such as NtnG2, Gnb4 and Gng2[20, 28], and found all these genes were significantly downregulated in CLA (and/or dEn neurons) of both EmxCre (Fig. 2A-C and 2A'-C') and NexCre (Fig. S5C-E) mutant brains. Furthermore, single cell mRNA sequencing (scmRNA-seq) of claustro-insular tissues revealed a large

spectrum of misregulated genes in Nurr1 deficient brains (see below, Fig. 5, S8 and S9), among which, Rgs20, for instance, was selectively attenuated in CLA, but not in Sp (Fig. 2D-D'). These results strongly indicate the specific genetic profile of CLA is altered by Nurr1 deficiency. Secondly, we tested if Nurr1 deficient CLA cells give rise to InC gene expression thereupon their ectopic localization. Cyp26b1 is a widely accepted InC marker[29, 30]. We quantified the proportion of Nurr1/Cyp26b1 double positive (Nurr1+/Cyp26b1+) cells relative to total Nurr1+ cells in claustro-insular region. While few Nurr1+/Cyp26b1+ cells were detected in controls, a considerably increased portion of Nurr1-Cterm+ cells (by ~9.70 ± 1.64 folds, $p = 0.00010$, ***) in the InC of EmxCre mutant brains switched on Cyp26b1 expression (Fig. 2E). By the same token, we quantified the proportions of Nurr1+/Neurod1+ and Nurr1+/Rorβ+ cells in claustro-insular region as Neurod1 and Rorβ are also preferentially expressed in InC cells but not in CLA *(Allen brain atlas*). The proportions of Nurr1+/Neurod1+ and Nurr1+/Rorβ+ cells are increased by ~4.49 ± 0.36 folds ($p < 0.0001$, ****) and by ~19.92 ± 0.72 folds ($p < 0.0001$, ****) in EmxCre mutant brains relative to those of control brains, respectively (Fig. 2F, 2G). Furthermore, the expression levels of these InC enriched genes in Nurr1 NexCre mutant brains are elevated to the comparable levels as those in EmxCre mutant brains (Fig. 2E-G). These results suggest Nurr1 deficient CLA cells tend to convert their genetic program to InC cells' postmitotically.

Axonal projection pattern is closely linked with their neuronal identity and distinct gene expression[31]. To test if the axonal projection pathways of Nurr1 deficient neurons are also altered accordingly, we performed retrograde axonal tracing by placing DiI crystals into two target regions – primary motor cortex (PMC, telencephalic) and hypothalamus (HT, diencephalic), which were reported to be connected intensively with InC, but very weakly with CLA[6, 32-36]. While efferent neurons to PMC are rarely rooted in CLA in control brains, Nurr1 deficient cell somas in InC frequently colocalize with DiI retrograde signals, supported by that the ratio of Nurr1+/DiI+ cells in Nurr1 deficient brains is increased by ~28.58 ± 4.53 folds compared with that in controls (Fig. S6A). Likewise, the ratio of Nurr1-Cterm+/DiI+ cells in mutant brains is approximately triple of that in controls in the scenario of HT labeling (Fig. S6B). Taken together, Nurr1 plays a decisive role in CLA cell identity establishment.

Functional connectivity associated with claustrum is disrupted in Nurr1 deficient mice

Given Nurr1's role in axonal wiring as above and wide interconnection of CLA neurons, we thus studied if connectivity mapping in Nurr1 deficient mice is altered using resting state functional magnetic resonance imaging (rs-fMRI). We first analyzed the functional connectivity (FC) of 17 cerebral networks (see "*Materials and Methods*") that have been reported to be connected to CLA[6, 35, 36], and found that the amygdala and prefrontal cortex (PFC) networks in Nurr1 deficient mice were the most affected compared with those of control mice (Fig. 3A), supported by their significantly lower values of independent component weight (Fig. 3B, 3C). In order to find out if the compromised plasticity in these networks is specifically correlated to CLA, we employed the method of seed-based differential mapping according to *Allen brain atlas*[8]. When both ipsilateral and contralateral CLA was seeded as the regions of interest (ROI), synchronous activity was strongly detected in amygdala and PFC networks in control brains, but considerably weakened in Nurr1 deficient brains (Fig. 3D-D'), suggesting the impaired FC in these networks of Nurr1 deficient brains is linked with CLA abnormality. Analysis based on single hemispheric CLA seed does not only depicted similar results (sagittal plane, Fig. 3E-E'), but also revealed that CLA is correlated to interhemispheric FC of amygdala and PFC networks, however, both are reduced in Nurr1 deficient brains (coronal plane, Fig. 3E-E').

Nurr1 deficient mice is more resistant to stress-elicited behavioral responses

Neural circuit between amygdala and CLA contributes to modulating responsive behaviors to stresses in rodents[9]. Given the genetic disturbance of CLA and impaired amygdala-CLA communication in Nurr1 deficient mice, we reasoned if Nurr1 is involved in regulation of stress-induced cognitive processing. We first tested control and Nurr1 deficient mice with elevated plus maze (EPM). Nurr1 deficient mice exhibited significantly longer travelling time and distance as well as higher velocity and visit frequency in the open arms of EPM than control mice (Fig. 4A-C, 4F and Fig. S7A). Moreover, Nurr1 deficient mice spent less time in closed arms of EPM than controls despite their similar moving distances (Fig. 4E, 4H). These results implicate Nurr1 deficient mice become less anxious to external stressors. We also defined the open arm ledges (10 cm) as high risk zones[37, 38], and found that Nurr1 deficient mice were more exploratory as they visited more often the risk zones and travelled longer time and distance in this area than control mice (Fig. 4D, 4G and Fig. S7B), indicating Nurr1 deficient mice are more resistant to the fear of taking risk. We next assessed animals'

anxiety induced by new environment using open field (OF). Nurr1 deficient mice travelled longer time and distance (Fig. 4J, 4K), and exhibited greater locomotion (Fig. S7D) in the central zone of OF than control mice in spite of their statistically indistinguishable velocity and visit frequency (Fig. S7E, S7F), strengthening the conclusions of EPM assay. Collectively, genetic abolishment of CLA ensemble by Nurr1 deficiency makes rodents more immune to stress-elicited emotional responses, such as anxiety and fear.

Transcriptomic profile of claustral neurons regulated by Nurr1

We next aimed to screen downstream effectors of Nurr1 that regulate CLA neuron activities. We isolated the anterior claustro-insular portions of control and Nurr1 deficient cortices (excluding posterior Nurr1+ Sb and entorhinal cortex), which were immediately subject to scmRNA-seq. We first generated a heatmap for genes regulated by Nurr1 and found that a wide spectrum of genes altered their expression patterns in Nurr1 deficient mice, particularly in L6-IT cluster (layer 6 intratelencephalon projecting glutamatergic neurons including CLA and dEn cells in Azimuth annotation[39]) (Fig. 5A). ISH for a number of top-rated genes in heatmap validated the specificity of our transcriptomic mapping (Fig. S8). Uniform manifold approximation and projection (UMAP) dimensionality reduction in combination with cell subclass clustering analysis for all cells provided a blueprint of claustro-insular cell heterogeneity, showing that the distribution of control and Nurr1 deficient cells is largely overlapping in glutamatergic neuron clusters besides L6-IT cluster (Fig. 5B, 5C). UMAP analysis based on Nurr1+ subpopulations revealed that Nurr1 expression was mainly detected in L2/3 (most likely Arimatsu cells), L6-IT (CLA and dEn) and L6b (Sp) clusters in controls (Fig. 5D, 5E), supported by ISH and cell type specific UAMP (Fig. S1, S8 and S9A). However, a large population of L6-IT cluster cells were no long recognizable in the absence of Nurr1 (red arrowheads in Fig. 5B, 5D), arguing their cell identity shift. Additionally, quite a few CLA-enriched markers, as shown in previous reports[20, 40, 55], are verified to be downregulated, but Rorβ is upregulated in our data (Fig. 5F), consistent with our molecular characterization.

Claustral cell positioning relies on suppression of Gαs-PKA signaling by Nurr1

Quite a few numbers of top-rated Nurr1 downstream genes in our transcriptomics were found linked with inhibition of G-protein signaling in developing CLA, such as Gnb4 and Gnb2 (Fig. 2, Fig. 5 and Fig. S9). Additionally, Gng2 (Gγ2), another reduced marker in CLA

neurons (Fig. 2B-B'), can heterodimerize with Gnb2/4 (Gβ2/4) to stabilize the silent Gα effectors[41, 42]. We thus hypothesized that low activity of Gα subunits might be vital for CLA development. To test this, we established a gain-of-function strategy by *in utero* electroporation (IUE) to restore targeted genes in CLA cells at E12.5 (Fig. S10), when the birth peak of mouse CLA neurons is[43]. We first electroporated GFP into control and Nurr1 deficient brains as references and quantified the proportions of Nurr1+/GFP+ cells positioned in CLA area relative to the total double positive cells. While Nurr1+/GFP+ cells were mainly populated in CLA of GFP-electroporated control brains (≈89.94%), only a small fraction of Nurr1-Cterm+/GFP+ cells were still resident in the CLA of GFP-electroporated Nurr1 deficient brains (≈15.44%). Instead, the majority of Nurr1-Cterm+/GFP+ cells in mutant brains were detected in InC area, consistent with their phenotypes in the non-electroporated hemispheres (Fig. 6A, 6B). We then analyzed Nurr1-GFP bicistronically electroporated mutant brains, showing that Nurr1 restoration in Nurr1 deficient CLA cells prevents most of Nurr1+/GFP+ cells from migrating to InC (≈69.63% in CLA) (Fig. 6A, 6B). The fraction should be even larger given some non-CLA cells carrying enforced Nurr1 expression were counted into denominator. Notably, co-electroporation of Gnb4- and Gng2-GFP into Nurr1 deficient brains increases the proportion of Nurr1-Cterm+/GFP+ cells in CLA by ~2.23 ± 0.24 folds ($p < 0.0001$, ****) relative to GFP-electroporated mutant brains (Fig. 6A, 6B). These results reveal restoration of Gα deactivators in Nurr1 deficient CLA cells facilitates their settlement in CLA territory.

Gα effector proteins are divided into a few subclasses, such as Gαs, Gαi, Gαq and $G\alpha_{12/13}$, to mediate distinctive cell actions, among which homeostasis of Gαs and Gαi cascades primarily regulates cell motility[44]. In order to further study the effect of Gα downstream cascades on CLA cell behaviors, we combined brain slice culture with acute pharmacological treatment. The brain slices were prepared from E15.5 embryos, cultured in supporting media for six days and then fixed by 4% paraformaldehyde[45]. The resulted tissues appeared morphologically intact. Nurr1+ CLA cells in untreated control tissues dwelled normally between Tle4+ striatal and InC DL neurons, while the majority of Nurr1-Cterm+ cells in untreated mutant slices migrated across InC DL neurons towards the pia, in agreement with the phenotype by Nurr1 deficiency *in vivo* (Fig. 6C). We then quantified the proportions of Nurr1-expressing cells positioned in CLA or InC relative to the total numbers. There was a

huge fraction (≈92.29%) of Nurr1+ cells in the CLA of untreated control slices in contrast to merely ≈8.78% Nurr1-Cterm+ cells in the CLA of untreated Nurr1 deficient slices (Fig. 6D). We next constantly treated Nurr1 deficient slices with NF449, a Gαs-specific cell-permeable inhibitor[46,47], and found a visibly larger fraction of Nurr1-Cterm+ cells ceasing prior to InC DL neurons (≈57.74%) (Fig. 6C, 6D). On the other hand, the treatment with pertussis toxin (PT), a Gαi-specific inhibitor[48, 49], to Nurr1 deficient slices did not exhibit such an effect as NF449 treatment did (Fig. 6C, 6D). Collectively, excessive activity of Gαs signaling in Nurr1 deficient CLA neurons causes, at least in part, their constitutive migration.

PKA signaling, as the most common downstream cascade of Gαs[44, 50], was assumed to be activated in the context of Nurr1 deficient cells. We indeed found the phosphorylation levels of PKA substrates, but not PKC substrates (Fig. S11A), ectopically surged up in Nurr1 deficient neurons (≈69.13%) in contrast to its barely detectable level in control brains (≈2.06%) (Fig. 6E, 6F). Interestingly, one of catalytic subunits of PKA complex, *Prcacb,* is upregulated in InC (Fig. S11B) but one regulatory subunit, *Prkar2b*, is downregulated in Nurr1 deficient brains (Fig. S9G). To investigate if CLA cell dislocation in Nurr1 deficient brains is linked with ectopic PKA activities, we prepared brain slice cultures from two hemispheres of the same brain and treated them with or without a cell-permeable PKA inhibitor Rp-cAMP[51]. PKA inhibition by Rp-cAMP enables a significantly larger population of Nurr1-Cterm+ cells resident in CLA area in the treated Nurr1 deficient hemispheres (≈59.30%) than that of non-treated ones (≈13.96%), mimicking the situation of NF449 treatment, suggesting minimal activity of Gαs-PKA signaling is critical for appropriate positioning of normal CLA neurons.

Discussion

There has been a long-term discussion on if CLA is the main processor for mammalian consciousness, inviting constantly growing interest in CLA studies in the last two decades. CLA has been confirmed to be the mostly interconnected tissue in brains to modulate a wide range of sophisticated behaviors as described above. However, the molecular mechanisms underlying CLA formation and physiological functions remain little known. Here we report one piece of earliest experimental evidences that Nurr1 is a master regulator to orchestrate CLA morphogenesis, cell identity establishment, FC networks and relevant behaviors.

The evo-devo relation between CLA and InC, and CLA cell migration path were not in agreement until Charles Watson and Luis Puelles proposed the latest descriptive model based on Nurr1 expression pattern, hypothesizing that principal CLA neurons derived from lateral pallial progenitors (LPP) first populate ventrally to Sp via radial migration and later coming cells from LPP bypass CLA to form InC in a typical inside-out manner[1, 19], but direct experimental evidence for this model still lacks. Here we confirm this theory using our mouse model where CLA cells deficient for Nurr1 transcription regulation constitutively migrate radially along Nestin+ glia into InC and are specified into InC-like cells. These results suggest CLA and InC derive from the same lineage and migrate along the same radial columns, and that Nurr1 is the decisive factor to segregate the earlier born clusters (mainly at E12.5)[43] to form subcortical CLA from the later born InC neurons. Nevertheless, we did not observe any tangentially migrating Nurr1-Cterm+ cells in mutant brains throughout our study, challenging their point of view that some Nurr1+ cells migrate dorsally to become Sp or Arimatsu cells. In contrast, Nurr1 deficient CLA cells constitutively migrate along a radial path and disconnected with intact Sp, raising a myth if CLA is truly a spatially continuous structure of Sp in spite of their partially common evolutionary origin[20].

Normal CLA territory has been described to be surrounded by striatum and Tle4+ InC DL neurons in mouse brains where a clear extreme capsule structure lacks[52]. CLA cells in Nurr1 deficient mice easily cross the fence to invade InC whereas surrounding DL cells appear to occupy original CLA territory. These results suggest there be mutually exclusive interaction between CLA and InC cells to assist claustro-insular organization. Nurr1 presides over CLA party and its deficiency alone can disrupt claustro-insular cytoarchitecture, marked by Cdh13 ISH. Notably, our scmRNA-seq data revealed quite a few cell-cell contact clues that are dysregulated by Nurr1 deficiency, such as molecules in ephrin-Eph and semaphorin-plexin signaling. These proteins are often axon membrane bound to mediate *trans* repelling interplay between contacted tissues[53, 54]. This may provide a molecular hint for how CLA is delineated by white matter (external and extreme capsules) in human brains.

Additionally, we found Nurr1 not only regulates CLA morphogenesis but also its cell fate specification, by showing that CLA signature genes are selectively downregulated while InC-expressing genes, such as Cyp26b1, Rorβ and Neurod1, are significantly upregulated in Nurr1 deficient CLA cells. Consistently, single cell transcriptomic analysis verified our

molecular characterization, and further reveal that CLA specific genetic program is broadly affected by Nurr1 deficiency. Moreover, another group also reported similar transcriptomic results when we were preparing the manuscript[55]. These independent studies therefore confirmed the same conclusion that Nurr1 is a key player to program CLA identity. Remarkably, not all cells derived from LPP carrying Nurr1 overexpression by IUE were converted into CLA neurons, suggesting that Nurr1 alone be necessary but not sufficient to determine CLA cell identity. Nurr1 is also strongly expressed in Sp and Sb, but its absence does not appear to affect their cell identity or anatomic structure. Nurr1's decisive role in cell fate is cell type- or region-specific.

Nurr1 expression has been detected in both cortical progenitors and CLA neurons in early brain development (*Allen brain atlas*), proposing a question if Nurr1 governs CLA cell activities pre- or postmitotically. We answered this question by genetic depletion of Nurr1 at distinct stages. Nurr1 inactivation in postmitotic neurons (Nex-Cre) could fully recapitulate the CLA developmental phenotypes as those when Nurr1 was inactivated in progenitors (Emx-Cre), suggesting a postmitotic mechanism of Nurr1 in the context of CLA formation. Moreover, IUE of GFP into wild type brains (Fig. S10) shows that Nurr1 expression is not present in CLA cells during migration from VZ to CP, indicating that Nurr1 expression was separated into two stages during CLA development – progenitor and neuronal, and that Nurr1 expression in progenitors is dispensable for cell migration towards CLA but its later expression in neuronal stage is the key for CLA morphogenesis.

Nurr1 is not only critical for CLA development, also for CLA-linked inter-areal connectivity organization. For instance, fMRI analysis seeding CLA as ROI showed synchronized activity of amygdala network is impaired in Nurr1 deficient mice. Recent report showed that stress responsive behaviors controlled by amygdala rely on CLA ensemble as part of processing circuit[9]. To test the idea if normal CLA cytoarchitecture and FC regulated by Nurr1 is essential for CLA dependent behaviors, we assessed our mice by EPM and OF assays. Nurr1 deficient mice were clearly more insensitive to stress-elicited emotional responses, consistent with their argument that CLA neuron inactivation led to increased resilience to stressors[9]. Taken together, Nurr1 is seated high in genetic hierarchy in CLA to dictate its entire development-connectivity-behavior dimension, in line with its life-long expression in CLA.

Immense evidence has shown G-protein mediated signaling is one of major regulatory pathways in cell motility, but Gα subclass effectors play complex and contextually divergent roles in variable cell types[56]. Both Gαs and Gαi isoforms have been shown to stimulate promigratory events in certain cell types but suppress cell migration in other circumstances, depending on their expression levels, homeostasis of Gαs/Gαi, and cell type-specific niche[56-61]. We therefore utilize selective inhibitors to reveal Gαs-PKA axis to be involved in the context of CLA cell ectopic migration caused by Nurr1 deficiency. Intracellular PKA pathway, as a main responsive signaling of Gαs, serves as a central paradigm to regulate cytoskeleton dynamics so as to coordinate almost all key events of cell migration, such as polarization, adhesive interaction with extracellular matrix, leading edge formation and soma translocation[62, 63]. Despite the delicate spatio-temporal control of PKA signaling in a motile cell in terms of its abundance, equilibrium of catalytic and regulatory subunits, activation timing and subcellular compartmentation, basic PKA activity is generally required[62-65]. In this regard, to simply minimize intracellular PKA activity may be the most cost-efficient implementation to ensure cell motionless. Nurr1 sets serial barriers at transcription level to keep PKA activity beneath threshold, such as upstream repressors and PKA subunits. Consistently, PKA substrate phosphorylation was strongly detected in radially migrating neocortical neurons, but selectively absent in static CLA cells.

Given the deep position and tight interplay with neighboring tissues of CLA (and dEn) in mouse brains, cell type-specific Cre line logically serves as a better tool for genetic study than artificial lesions[66], which debilitates complete and neat gene inactivation in CLA cells. However, the CLA-specific Cre lines that have been reported in an experiment so far trigger recombination either in a relatively small subset of CLA neurons (Egr2-Cre) or only in adult CLA (Tbx21-Cre)[10, 67, 68]. Our study would open a new window for cell type-specific investigation of CLA (and dEn) in the future.

References

1. Puelles L, Ayad A, Alonso A, Sandoval JE, MartÍnez-de-la-Torre M, Medina L, Ferran JL. Selective early expression of the orphan nuclear receptor Nr4a2 identifies the claustrum

homolog in the avian mesopallium: Impact on sauropsidian/mammalian pallium comparisons. J Comp Neurol. 2016 Feb 15;524(3):665-703. doi: 10.1002/cne.23902.

2. Norimoto H, Fenk LA, Li HH, Tosches MA, Gallego-Flores T, Hain D, Reiter S, Kobayashi R, Macias A, Arends A, Klinkmann M, Laurent G. A claustrum in reptiles and its role in slow-wave sleep. Nature. 2020 Feb;578(7795):413-418. doi: 10.1038/s41586-020-1993-6.
3. Baizer JS, Sherwood CC, Noonan M, Hof PR. Comparative organization of the claustrum: what does structure tell us about function? Front Syst Neurosci. 2014 Jul 2;8:117. doi: 10.3389/fnsys.2014.00117.
4. Smith JB, Lee AK, Jackson J. The claustrum. Curr Biol. 2020 Dec 7;30(23):R1401-R1406. doi: 10.1016/j.cub.2020.09.069.
5. Crick FC, Koch C. What is the function of the claustrum? Philos Trans R Soc Lond B Biol Sci. 2005 Jun 29;360(1458):1271-9. doi: 10.1098/rstb.2005.1661.
6. Wang Q, Ng L, Harris JA, Feng D, Li Y, Royall JJ, Oh SW, Bernard A, Sunkin SM, Koch C, Zeng H. Organization of the connections between claustrum and cortex in the mouse. J Comp Neurol. 2017 Apr 15;525(6):1317-1346. doi: 10.1002/cne.24047.
7. Krimmel SR, White MG, Panicker MH, Barrett FS, Mathur BN, Seminowicz DA. Resting state functional connectivity and cognitive task-related activation of the human claustrum. Neuroimage. 2019 Aug 1;196:59-67. doi: 10.1016/j.neuroimage.2019.03.075.
8. Qadir H, Stewart BW, VanRyzin JW, Wu Q, Chen S, Seminowicz DA, Mathur BN. The mouse claustrum synaptically connects cortical network motifs. Cell Rep. 2022 Dec 20;41(12):111860. doi: 10.1016/j.celrep.2022.111860.
9. Niu M, Kasai A, Tanuma M, Seiriki K, Igarashi H, Kuwaki T, Nagayasu K, Miyaji K, Ueno H, Tanabe W, Seo K, Yokoyama R, Ohkubo J, Ago Y, Hayashida M, Inoue KI, Takada M, Yamaguchi S, Nakazawa T, Kaneko S, Okuno H, Yamanaka A, Hashimoto H. Claustrum mediates bidirectional and reversible control of stress-induced anxiety responses. Sci Adv. 2022 Mar 18;8(11):eabi6375. doi: 10.1126/sciadv.abi6375.
10. Atlan G, Terem A, Peretz-Rivlin N, Sehrawat K, Gonzales BJ, Pozner G, Tasaka GI, Goll Y, Refaeli R, Zviran O, Lim BK, Groysman M, Goshen I, Mizrahi A, Nelken I, Citri A. The

Claustrum Supports Resilience to Distraction. Curr Biol. 2018 Sep 10;28(17):2752-2762.e7. doi: 10.1016/j.cub.2018.06.068.

11. White MG, Panicker M, Mu C, Carter AM, Roberts BM, Dharmasri PA, Mathur BN. Anterior Cingulate Cortex Input to the Claustrum Is Required for Top-Down Action Control. Cell Rep. 2018 Jan 2;22(1):84-95. doi: 10.1016/j.celrep.2017.12.023.
12. Chevée M, Finkel EA, Kim SJ, O'Connor DH, Brown SP. Neural activity in the mouse claustrum in a cross-modal sensory selection task. Neuron. 2022 Feb 2;110(3):486-501.e7. doi: 10.1016/j.neuron.2021.11.013.
13. Atlan G, Matosevich N, Peretz-Rivlin N, Marsh-Yvgi I, Zelinger N, Chen E, Kleinman T, Bleistein N, Sheinbach E, Groysman M, Nir Y, Citri A. Claustrum neurons projecting to the anterior cingulate restrict engagement during sleep and behavior. Nat Commun. 2024 Jun 26;15(1):5415. doi: 10.1038/s41467-024-48829-6.
14. Atilgan H, Doody M, Oliver DK, McGrath TM, Shelton AM, Echeverria-Altuna I, Tracey I, Vyazovskiy VV, Manohar SG, Packer AM. Human lesions and animal studies link the claustrum to perception, salience, sleep and pain. Brain. 2022 Jun 3;145(5):1610-1623. doi: 10.1093/brain/awac114.
15. White MG, Panicker M, Mu C, Carter AM, Roberts BM, Dharmasri PA, Mathur BN. Anterior Cingulate Cortex Input to the Claustrum Is Required for Top-Down Action Control. Cell Rep. 2018 Jan 2;22(1):84-95. doi: 10.1016/j.celrep.2017.12.023.
16. Jackson J, Karnani MM, Zemelman BV, Burdakov D, Lee AK. Inhibitory Control of Prefrontal Cortex by the Claustrum. Neuron. 2018 Sep 5;99(5):1029-1039.e4. doi: 10.1016/j.neuron.2018.07.031.
17. Zetterström RH, Solomin L, Jansson L, Hoffer BJ, Olson L, Perlmann T. Dopamine neuron agenesis in Nurr1-deficient mice. Science. 1997 Apr 11;276(5310):248-50. doi: 10.1126/science.276.5310.248.
18. Kadkhodaei B, Ito T, Joodmardi E, Mattsson B, Rouillard C, Carta M, Muramatsu S, Sumi-Ichinose C, Nomura T, Metzger D, Chambon P, Lindqvist E, Larsson NG, Olson L, Björklund A, Ichinose H, Perlmann T. Nurr1 is required for maintenance of maturing and adult midbrain dopamine neurons. J Neurosci. 2009 Dec 16;29(50):15923-32. doi: 10.1523/JNEUROSCI.3910-09.2009.

19. Watson C, Puelles L. Developmental gene expression in the mouse clarifies the organization of the claustrum and related endopiriform nuclei. J Comp Neurol. 2017 Apr 15;525(6):1499-1508. doi: 10.1002/cne.24034.

20. Bruguier H, Suarez R, Manger P, Hoerder-Suabedissen A, Shelton AM, Oliver DK, Packer AM, Ferran JL, García-Moreno F, Puelles L, Molnár Z. In search of common developmental and evolutionary origin of the claustrum and subplate. J Comp Neurol. 2020 Dec 1;528(17):2956-2977. doi: 10.1002/cne.24922.

21. Gorski JA, Talley T, Qiu M, Puelles L, Rubenstein JL, Jones KR. Cortical excitatory neurons and glia, but not GABAergic neurons, are produced in the Emx1-expressing lineage. J Neurosci. 2002 Aug 1;22(15):6309-14. doi: 10.1523/JNEUROSCI.22-15-06309.2002.

22. García-Yagüe ÁJ, Rada P, Rojo AI, Lastres-Becker I, Cuadrado A. Nuclear import and export signals control the subcellular localization of Nurr1 protein in response to oxidative stress. J Biol Chem. 2013 Feb 22;288(8):5506-17. doi: 10.1074/jbc.M112.439190.

23. Hoerder-Suabedissen A, Molnár Z. Molecular diversity of early-born subplate neurons. Cereb Cortex. 2013 Jun;23(6):1473-83. doi: 10.1093/cercor/bhs137.

24. Arlotta P, Molyneaux BJ, Chen J, Inoue J, Kominami R, Macklis JD. Neuronal subtype-specific genes that control corticospinal motor neuron development in vivo. Neuron. 2005 Jan 20;45(2):207-21. doi: 10.1016/j.neuron.2004.12.036.

25. Xie Z, Ma X, Ji W, Zhou G, Lu Y, Xiang Z, Wang YX, Zhang L, Hu Y, Ding YQ, Zhang WJ. Zbtb20 is essential for the specification of CA1 field identity in the developing hippocampus. Proc Natl Acad Sci U S A. 2010 Apr 6;107(14):6510-5. doi: 10.1073/pnas.0912315107.

26. Nielsen JV, Thomassen M, Møllgård K, Noraberg J, Jensen NA. Zbtb20 defines a hippocampal neuronal identity through direct repression of genes that control projection neuron development in the isocortex. Cereb Cortex. 2014 May;24(5):1216-29. doi: 10.1093/cercor/bhs400.

27. Goebbels S, Bormuth I, Bode U, Hermanson O, Schwab MH, Nave KA. Genetic targeting of principal neurons in neocortex and hippocampus of NEX-Cre mice. Genesis. 2006 Dec;44(12):611-21. doi: 10.1002/dvg.20256.

28. Watakabe A. In situ hybridization analyses of claustrum-enriched genes in marmosets. J Comp Neurol. 2017 Apr 15;525(6):1442-1458. doi: 10.1002/cne.24021.

29. Puelles L. Current Status of the Hypothesis of a Claustro-Insular Homolog in Sauropsids. Brain Behav Evol. 2022;96(4-6):212-241. doi: 10.1159/000520742.

30. Christianson JP. An Insula-Enriched Regulator of Retinoic Acid Marks a New Intersection in the Neural Circuitry of Mouse Social Behavior. Am J Psychiatry. 2023 Apr 1;180(4):262-264. doi: 10.1176/appi.ajp.20230110.

31. Greig LC, Woodworth MB, Galazo MJ, Padmanabhan H, Macklis JD. Molecular logic of neocortical projection neuron specification, development and diversity. Nat Rev Neurosci. 2013 Nov;14(11):755-69. doi: 10.1038/nrn3586.

32. Gehrlach DA, Weiand C, Gaitanos TN, Cho E, Klein AS, Hennrich AA, Conzelmann KK, Gogolla N. A whole-brain connectivity map of mouse insular cortex. Elife. 2020 Sep 17;9:e55585. doi: 10.7554/eLife.55585.

33. Nikolenko VN, Rizaeva NA, Beeraka NM, Oganesyan MV, Kudryashova VA, Dubovets AA, Borminskaya ID, Bulygin KV, Sinelnikov MY, Aliev G. The mystery of claustral neural circuits and recent updates on its role in neurodegenerative pathology. Behav Brain Funct. 2021 Jul 7;17(1):8. doi: 10.1186/s12993-021-00181-1.

34. Wright H, Li X, Fallon NB, Crookall R, Giesbrecht T, Thomas A, Halford JC, Harrold J, Stancak A. Differential effects of hunger and satiety on insular cortex and hypothalamic functional connectivity. Eur J Neurosci. 2016 May;43(9):1181-9. doi: 10.1111/ejn.13182.

35. Zingg B, Dong HW, Tao HW, Zhang LI. Input-output organization of the mouse claustrum. J Comp Neurol. 2018 Oct 15;526(15):2428-2443. doi: 10.1002/cne.24502.

36. Wang Q, Wang Y, Kuo HC, Xie P, Kuang X, Hirokawa KE, Naeemi M, Yao S, Mallory M, Ouellette B, Lesnar P, Li Y, Ye M, Chen C, Xiong W, Ahmadinia L, El-Hifnawi L, Cetin A, Sorensen SA, Harris JA, Zeng H, Koch C. Regional and cell-type-specific afferent and efferent projections of the mouse claustrum. Cell Rep. 2023 Feb 28;42(2):112118. doi: 10.1016/j.celrep.2023.112118.

37. Fernandes C, File SE. The influence of open arm ledges and maze experience in the elevated plus-maze. Pharmacol Biochem Behav. 1996 May;54(1):31-40. doi: 10.1016/0091-3057(95)02171-x.

38. Horii Y, Kawaguchi M. Higher detection sensitivity of anxiolytic effects of diazepam by ledge-free open arm with opaque walled closed arm elevated plus maze in male rats. Behav Brain Res. 2015 Nov 1;294:131-40. doi: 10.1016/j.bbr.2015.07.059.

39. Yao Z, Liu H, Xie F, Fischer S, Adkins RS, Aldridge AI, Ament SA, Bartlett A, Behrens MM, Van den Berge K, Bertagnolli D, de Bézieux HR, Biancalani T, Booeshaghi AS, Bravo HC, Casper T, Colantuoni C, Crabtree J, Creasy H, Crichton K, Crow M, Dee N, Dougherty EL, Doyle WI, Dudoit S, Fang R, Felix V, Fong O, Giglio M, Goldy J, Hawrylycz M, Herb BR, Hertzano R, Hou X, Hu Q, Kancherla J, Kroll M, Lathia K, Li YE, Lucero JD, Luo C, Mahurkar A, McMillen D, Nadaf NM, Nery JR, Nguyen TN, Niu SY, Ntranos V, Orvis J, Osteen JK, Pham T, Pinto-Duarte A, Poirion O, Preissl S, Purdom E, Rimorin C, Risso D, Rivkin AC, Smith K, Street K, Sulc J, Svensson V, Tieu M, Torkelson A, Tung H, Vaishnav ED, Vanderburg CR, van Velthoven C, Wang X, White OR, Huang ZJ, Kharchenko PV, Pachter L, Ngai J, Regev A, Tasic B, Welch JD, Gillis J, Macosko EZ, Ren B, Ecker JR, Zeng H, Mukamel EA. A transcriptomic and epigenomic cell atlas of the mouse primary motor cortex. Nature. 2021 Oct;598(7879):103-110. doi: 10.1038/s41586-021-03500-8.

40. Erwin SR, Bristow BN, Sullivan KE, Kendrick RM, Marriott B, Wang L, Clements J, Lemire AL, Jackson J, Cembrowski MS. Spatially patterned excitatory neuron subtypes and projections of the claustrum. Elife. 2021 Aug 16;10:e68967. doi: 10.7554/eLife.68967.

41. Rosskopf D, Nikula C, Manthey I, Joisten M, Frey U, Kohnen S, Siffert W. The human G protein beta4 subunit: gene structure, expression, Ggamma and effector interaction. FEBS Lett. 2003 Jun 5;544(1-3):27-32. doi: 10.1016/s0014-5793(03)00441-1.

42. Stallmeyer B, Kuß J, Kotthoff S, Zumhagen S, Vowinkel K, Rinné S, Matschke LA, Friedrich C, Schulze-Bahr E, Rust S, Seebohm G, Decher N, Schulze-Bahr E. A Mutation in the G-Protein Gene GNB2 Causes Familial Sinus Node and Atrioventricular Conduction Dysfunction. Circ Res. 2017 May 12;120(10):e33-e44. doi: 10.1161/CIRCRESAHA.116.310112.

43. Hoerder-Suabedissen A, Ocana-Santero G, Draper TH, Scott SA, Kimani JG, Shelton AM, Butt SJB, Molnár Z, Packer AM. Temporal origin of mouse claustrum and development of

its cortical projections. Cereb Cortex. 2023 Mar 21;33(7):3944-3959. doi: 10.1093/cercor/bhac318.

44. Jo M, Jung ST. Engineering therapeutic antibodies targeting G-protein-coupled receptors. Exp Mol Med. 2016 Feb 5;48(2):e207. doi: 10.1038/emm.2015.105.

45. Clegg JM, Pratt T. Organotypic Slice Culture of the Embryonic Mouse Brain. Bio Protoc. 2020 Jul 5;10(13):e3674. doi: 10.21769/BioProtoc.3674.

46. Zhang X, Candas M, Griko NB, Taussig R, Bulla LA Jr. A mechanism of cell death involving an adenylyl cyclase/PKA signaling pathway is induced by the Cry1Ab toxin of Bacillus thuringiensis. Proc Natl Acad Sci U S A. 2006 Jun 27;103(26):9897-902. doi: 10.1073/pnas.0604017103.

47. Lin P, Cheng T, Ma S, Gao J, Jin S, Jiang L, Xia Q. Bacillus bombysepticus α-Toxin Binding to G Protein-Coupled Receptor Kinase 2 Regulates cAMP/PKA Signaling Pathway to Induce Host Death. PLoS Pathog. 2016 Mar 29;12(3):e1005527. doi: 10.1371/journal.ppat.1005527.

48. Littler DR, Ang SY, Moriel DG, Kocan M, Kleifeld O, Johnson MD, Tran MT, Paton AW, Paton JC, Summers RJ, Schembri MA, Rossjohn J, Beddoe T. Structure-function analyses of a pertussis-like toxin from pathogenic Escherichia coli reveal a distinct mechanism of inhibition of trimeric G-proteins. J Biol Chem. 2017 Sep 8;292(36):15143-15158. doi: 10.1074/jbc.M117.796094.

49. Mangmool S, Kurose H. G(i/o) protein-dependent and -independent actions of Pertussis Toxin (PTX). Toxins (Basel). 2011 Jul;3(7):884-99. doi: 10.3390/toxins3070884.

50. Ramms DJ, Raimondi F, Arang N, Herberg FW, Taylor SS, Gutkind JS. Gαs-Protein Kinase A (PKA) Pathway Signalopathies: The Emerging Genetic Landscape and Therapeutic Potential of Human Diseases Driven by Aberrant Gαs-PKA Signaling. Pharmacol Rev. 2021 Oct;73(4):155-197. doi: 10.1124/pharmrev.120.000269.

51. Gjertsen BT, Mellgren G, Otten A, Maronde E, Genieser HG, Jastorff B, Vintermyr OK, McKnight GS, Døskeland SO. Novel (Rp)-cAMPS analogs as tools for inhibition of cAMP-kinase in cell culture. Basal cAMP-kinase activity modulates interleukin-1 beta action. J Biol Chem. 1995 Sep 1;270(35):20599-607. doi: 10.1074/jbc.270.35.20599.

52. Shaker T, Dagpa GJ, Cattaud V, Marriott BA, Sultan M, Almokdad M, Jackson J. A simple and reliable method for claustrum localization across age in mice. Mol Brain. 2024 Feb 17;17(1):10. doi: 10.1186/s13041-024-01082-w.

53. Halloran MC, Wolman MA. Repulsion or adhesion: receptors make the call. Curr Opin Cell Biol. 2006 Oct;18(5):533-40. doi: 10.1016/j.ceb.2006.08.010.

54. Rozbesky D, Jones EY. Cell guidance ligands, receptors and complexes - orchestrating signalling in time and space. Curr Opin Struct Biol. 2020 Apr;61:79-85. doi: 10.1016/j.sbi.2019.11.007.

55. Mantas I, Flais I, Masarapu Y, Ionescu T, Frapard S, Jung F, Le Merre P, Saarinen M, Tiklova K, Salmani BY, Gillberg L, Zhang X, Chergui K, Carlén M, Giacomello S, Hengerer B, Perlmann T, Svenningsson P. Claustrum and dorsal endopiriform cortex complex cell-identity is determined by Nurr1 and regulates hallucinogenic-like states in mice. Nat Commun. 2024 Sep 18;15(1):8176. doi: 10.1038/s41467-024-52429-9.

56. Cotton M, Claing A. G protein-coupled receptors stimulation and the control of cell migration. Cell Signal. 2009 Jul;21(7):1045-53. doi: 10.1016/j.cellsig.2009.02.008.

57. Surve CR, To JY, Malik S, Kim M, Smrcka AV. Dynamic regulation of neutrophil polarity and migration by the heterotrimeric G protein subunits Gαi-GTP and Gβγ. Sci Signal. 2016 Feb 23;9(416):ra22. doi: 10.1126/scisignal.aad8163.

58. Xu J, Wang F, Van Keymeulen A, Herzmark P, Straight A, Kelly K, Takuwa Y, Sugimoto N, Mitchison T, Bourne HR. Divergent signals and cytoskeletal assemblies regulate self-organizing polarity in neutrophils. Cell. 2003 Jul 25;114(2):201-14. doi: 10.1016/s0092-8674(03)00555-5.

59. Thompson BD, Jin Y, Wu KH, Colvin RA, Luster AD, Birnbaumer L, Wu MX. Inhibition of G alpha i2 activation by G alpha i3 in CXCR3-mediated signaling. J Biol Chem. 2007 Mar 30;282(13):9547-9555. doi: 10.1074/jbc.M610931200.

60. Wu VH, Yung BS, Faraji F, Saddawi-Konefka R, Wang Z, Wenzel AT, Song MJ, Pagadala MS, Clubb LM, Chiou J, Sinha S, Matic M, Raimondi F, Hoang TS, Berdeaux R, Vignali DAA, Iglesias-Bartolome R, Carter H, Ruppin E, Mesirov JP, Gutkind JS. The GPCR-Gαs-PKA signaling axis promotes T cell dysfunction and cancer immunotherapy failure. Nat Immunol. 2023 Aug;24(8):1318-1330. doi: 10.1038/s41590-023-01529-7.

61. Ramms DJ, Raimondi F, Arang N, Herberg FW, Taylor SS, Gutkind JS. Gαs-Protein Kinase A (PKA) Pathway Signalopathies: The Emerging Genetic Landscape and Therapeutic Potential of Human Diseases Driven by Aberrant Gαs-PKA Signaling. Pharmacol Rev. 2021 Oct;73(4):155-197. doi: 10.1124/pharmrev.120.000269.

62. Howe AK. Regulation of actin-based cell migration by cAMP/PKA. Biochim Biophys Acta. 2004 Jul 5;1692(2-3):159-74. doi: 10.1016/j.bbamcr.2004.03.005.

63. Newell-Litwa KA, Horwitz AR. Cell migration: PKA and RhoA set the pace. Curr Biol. 2011 Aug 9;21(15):R596-8. doi: 10.1016/j.cub.2011.06.032.

64. Svec KV, Howe AK. Protein Kinase A in cellular migration-Niche signaling of a ubiquitous kinase. Front Mol Biosci. 2022 Jul 22;9:953093. doi: 10.3389/fmolb.2022.953093.

65. Stoufflet J, Chaulet M, Doulazmi M, Fouquet C, Dubacq C, Métin C, Schneider-Maunoury S, Trembleau A, Vincent P, Caillé I. Primary cilium-dependent cAMP/PKA signaling at the centrosome regulates neuronal migration. Sci Adv. 2020 Sep 2;6(36):eaba3992. doi: 10.1126/sciadv.aba3992.

66. Gu T, Dong J, Ge J, Feng J, Liu X, Chen Y, Liu J. Neurotoxic lesions of the anterior claustrum influence cued fear memory in rats. Front Psychiatry. 2024 Apr 19;15:1387507. doi: 10.3389/fpsyt.2024.1387507.

67. Smith JB, Lee AK, Jackson J. The claustrum. Curr Biol. 2020 Dec 7;30(23):R1401-R1406. doi: 10.1016/j.cub.2020.09.069.

68. Narikiyo K, Mizuguchi R, Ajima A, Shiozaki M, Hamanaka H, Johansen JP, Mori K, Yoshihara Y. The claustrum coordinates cortical slow-wave activity. Nat Neurosci. 2020 Jun;23(6):741-753. doi: 10.1038/s41593-020-0625-7.

Acknowledgments:

We want to thank Rike Dannenberg, Denis Lajkó and Jutta Schüller for their brilliant technical support. NEX-Cre mice were kindly contributed by the group of KA Nave, Max-Planck-Institute of Experimental Medicine, Göttingen, Germany. Joseph Kuchling provided necessary assistance to upgrade the fMRI pipeline for seed-back analysis. We also want to thank Markus Aswendt for sharing the standard operating procedures for rs-fMRI anesthesia.

Funding:

1) As for molecular characterization of mouse model, sequencing and animal behavior tests: VT group was financially supported by German Research Foundation (DFG grant TA 303/14-1) and the Ministry of Science and Higher Education of the Russian Federation (project no. FSWR-2023-0029).
2) As for fMRI analysis: funding was provided by the German Federal Ministry of Education and Research (BMBF) under the ERA-NET NEURON scheme (01EW2305), and the German Research Foundation (DFG, project BO 4484/2-1, Project-ID 424778381-TRR 295 ReTune and EXC-2049-390688087 NeuroCure).

Author contributions:

Conceptualization: KY, VT

Methodology: KY established the cellular and surgical methods, such as brain slice culture, IUE, et al. KY and PL developed some of the molecular and cellular methods, such as ISH, IF and DiI, et al. AN analyzed the transcriptomic data. SM and MF performed fMRI examination. MM, CF and PBS introduced and upgraded the analytic pipeline of fMRI. SPK and PBS analyzed the fMRI data. KY, PD and ML developed the animal behaviors tests. KY, PL and PD performed genotyping.

Investigation: KY and PL performed molecular and cellular characterization for Nurr1 cKO mouse model. KY carried out IUE and brains slice culture experiments. KY isolated the cortical tissues and AN analyzed the scmRNA sequencing data. SM, MF, SPK and PBS contributed to the experimental line of fMRI. KY and PD performed animal behaviors tests under ML's supervision and KY analyzed the statistical data.

Funding acquisition: 1) Main funding of the project for molecular characterization of mouse model, sequencing and animal behavior tests was provided by VT; 2) funding for fMRI analysis was provided by PBS.

Supervision: KY, VT

Writing original draft and editing: KY, VT

Competing interests: All authors declare that they have no competing interests.

Data availability: All data in the main text and supplement supporting the scientific findings of this study will be made available on a central repository.

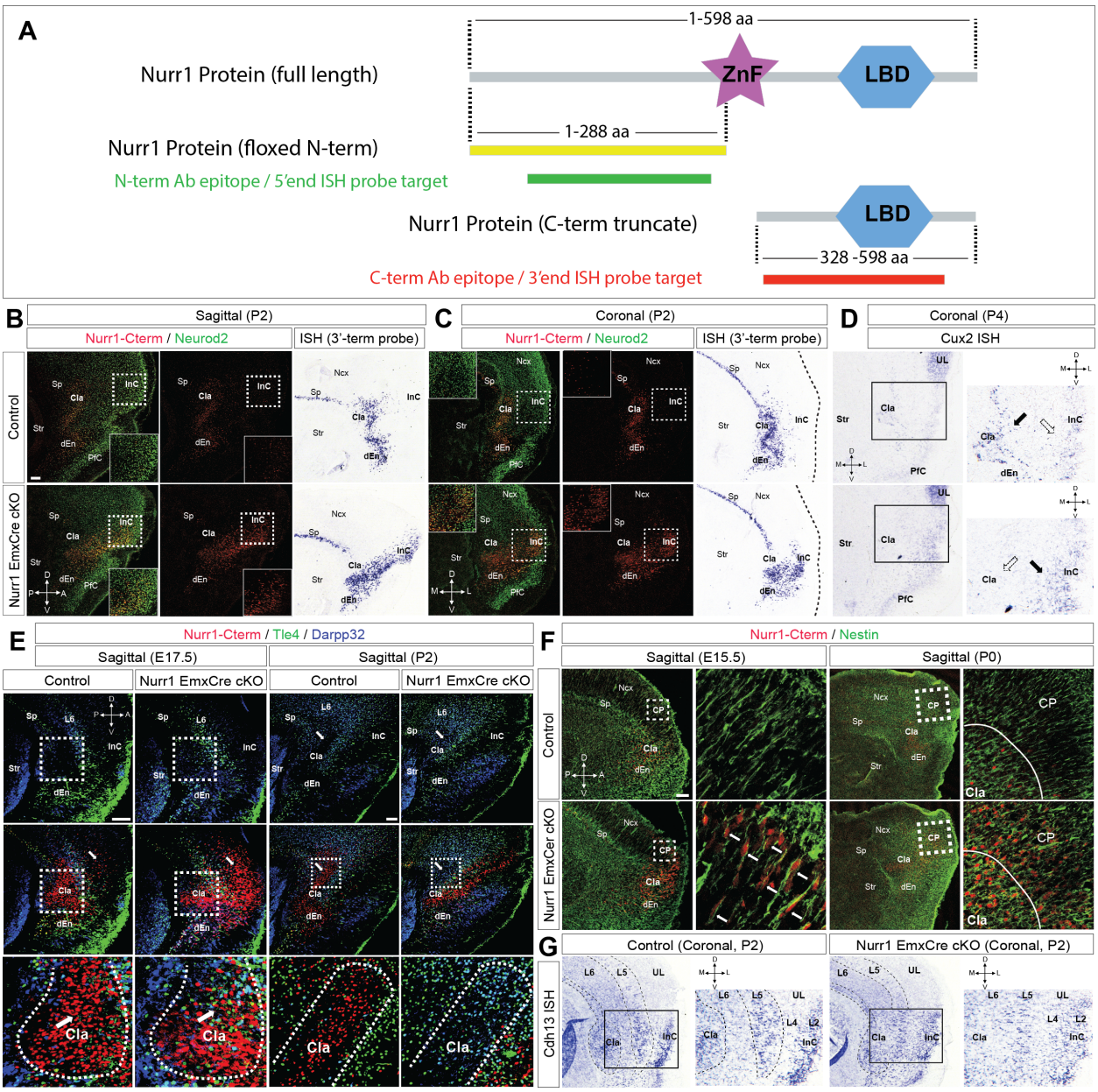

Figure 1 Nurr1 is a key regulator for claustrum morphogenesis.

(A) Illustration of Nurr1 molecular structure. The full-length (FL) Nurr1 protein consists of a DNA-binding zinc finger (ZnF) domain and a ligand-binding domain (LBD). The coding sequence of N-terminal region (Nterm, yellow, 1 – 288 amino acids (aa)) of Nurr1 protein is floxed (Kadkhodaei, et al., 2009). The truncated C-terminal portion (Cterm, red, 328 – 598 aa) of Nurr1 protein in the same original open reading frame loses ZnF domain after Cre-mediated recombination. The protein epitopes targeted by the antibodies (ab) or the transcript sequences targeted by the ISH probes are represented in green (Nterm ab or 5'end probe) and red (Cterm ab or 3'end probe), respectively.

(B, C) Immunofluorescence (IF) staining for Nurr1-Cterm (red) and Neurod2 (green) on sagittal (**B**) and coronal (**C**) sections of control and EmxCre+ Nurr1 deficient (cKO) brains at P2. Nurr1/Neurod2 double positive (Nurr1+/Neurod2+) claustral (CLA) neurons are mostly positioned between striatum (str) and insular cortex (InC), however, a huge population of Nurr1 deficient cells over-migrate in InC territory. ISH using the Nurr1-3'end probe on sagittal and coronal sections show the same migration deficits of Nurr1 deficient CLA cells as the IF data. The framed images show magnification views of the dotted-line boxed areas. Sp, subplate; dEn, dorsal endopiriform nucleus; PfC, piriform cortex, Ncx, neocortex. D, dorsal; A, anterior; V, ventral; P, posterior, M, medial; L, lateral. Scale bar: 200 μm (the same in this figure).

(D) ISH using the Cux2 probe on coronal sections of control and Nurr1 cKO brains at P2. Cux2 is strongly expressed in a subpopulation of CLA neurons (solid arrowhead) and weakly expressed in InC (hollow arrowhead), but its expression was ectopically detected in the InC of Nurr1 cKO brains but no longer in CLA, implying that Cux2+ CLA neurons over-migrate into InC. The enlarged images show magnification views of the boxed areas (the same below in all figures). UL, upper layers of Ncx.

(E) IF for Nurr1-Cterm (red), Tle4 (green) and Darpp32 (blue) on sagittal sections of control and EmxCre+ mutant brains at E17.5 and P2. CLA neurons are already largely ceased in the area surrounded by Tle4+/Darpp32+ deeper layer (DL) neurons at E17.5, and these DL neurons delineate the border for Nurr1+ CLA neurons at P2 in control brains. However, the majority of Nurr1 deficient CLA cells already migrate across Tle4+/Darpp32+ DL neurons at E17.5 and are eventually located in InC anterior to DL neurons at P2. The original CLA area is filled with Tle4+/Darpp32+ DL neurons in Nurr1 deficient brains. The arrowheads indicate CLA areas in control and cKO brains. The dotted lines delineate CLA territories from DL neurons.

(F) IF for Nurr1-Cterm (red) and Nestin (green) on sagittal sections of control and EmxCre+ mutant brains at E15.5 and P0. Nurr1 deficient CLA neurons always keep radial migration along Nestin+ radial glia. The lines in P0 images delineate the borders between CLA and Ncx. CP, cortical plate.

(G) ISH using the Cdh13 probe on coronal sections of control and EmxCre+ mutant brains at P2. The laminated expression of Cdh13 depicts the cortical cytoarchitecture in control brains by displaying its stronger expression in CLA, layer 5 (L5) and L2 of Ncx, but weaker expression in L6 and L4 along medio-lateral axis. However, the clear cytoarchitecture is disrupted by migrating Nurr1 deficient cells.

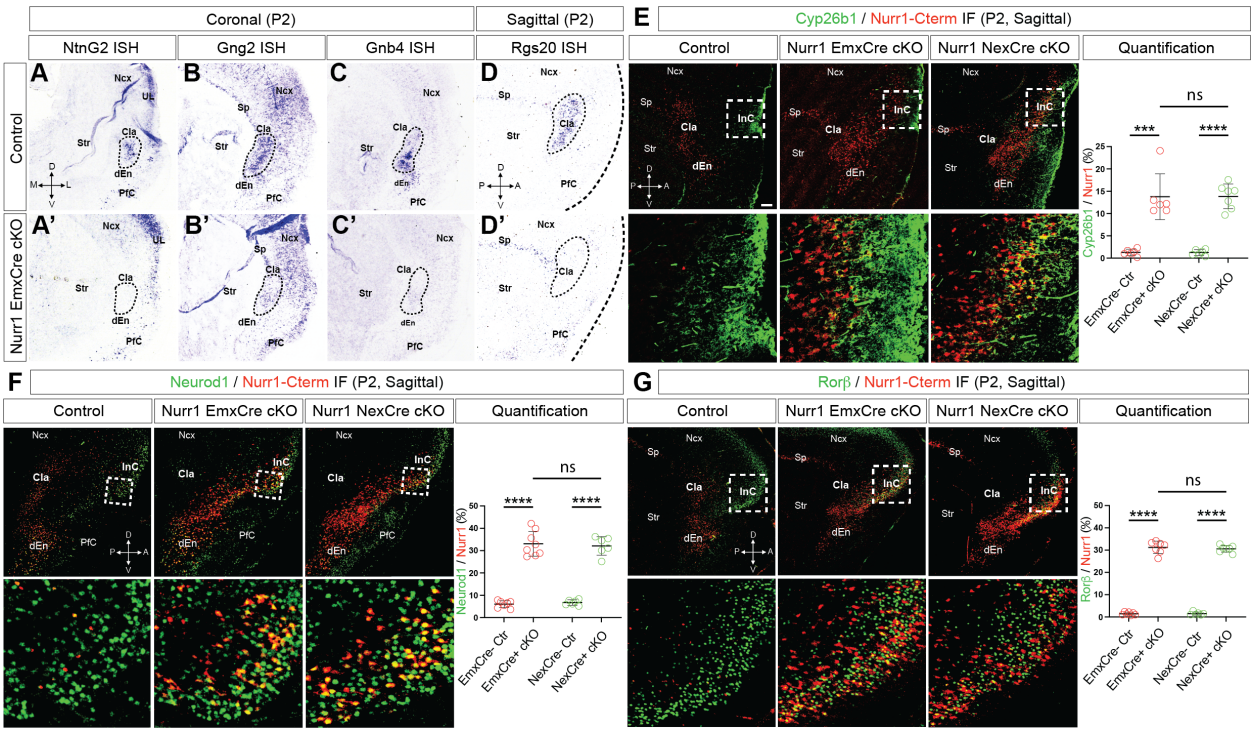

Figure 2 Nurr1 is essential to determine claustral cell fate.

(A-A' – D-D') ISH using the NtnG2, Gng2, Gnb4 and Rgs20 probes on brain sections of control and EmxCre+ mutant brains at P2. NtnG2 is expressed in CLA, UL and PfC in control brains but selectively downregulated in CLA of Nurr1 deficient brains (**A-A'**). Gng2 expression is widely detectable in CLA, Sp, PfC and Ncx in control brains (**B**), whereas its expression is severely reduced in ClA but not in surrounding areas of mutant brains (**B'**). Gnb4 is specifically expressed in CLA and dEn neurons in control brains (**C**) but becomes rarely detectable in Nurr1 deficient brains (**C'**). (**D-D'**) ISH using the Rgs20 probe on sagittal sections of control and EmxCre+ mutant brains at P2. Rgs20 is normally expressed in Sp and CLA but selectively absent in CLA in mutant brains. The dotted-line circles in (**A-A' – D-D'**) indicate CLA areas.

(E – G) IF for Nurr1-Cterm with Cyp26b1 (**E**), Neurod1 (**F**) and Rorβ (**G**) on sagittal sections of control, EmxCre+ and NexCre+ Nurr1 deficient brains at P2. Nurr1+/Cyp26b1+ cells are rarely detectable in control brains but significantly increased in both EmxCre+ and NexCre+ mutant brains (**E**). The proportion of Nurr1+/Cyp26b1+ cells in EmxCre+ mutant brains (≈13.77%, n = 6) is increased by ~9.70 ± 1.64 folds (p = 0.00010, ***) relative to controls (≈1.29%, n = 6). The proportion in NexCre+ cKO brains (≈13.85%, n = 7) is increased by ~9.95 ± 0.92 folds ($p < 0.0001$, ****) relative to controls (≈1.27%, n = 6), to the similar level with EmxCre+ mutant brains (p = 0.97, ns). The proportions of Nurr1+/Neurod1+ cells in EmxCre+ and NexCre+ mutant brains are

also elevated to similar levels ($p = 0.72$, ns): the proportion in EmxCre+ mutant brains (≈33.11%, n = 8) is increased by ~4.49 ± 0.36 folds ($p < 0.0001$, ****) relative to controls (≈ 6.03%, n = 7), and the proportion in NexCre+ cKO brains (≈32.09%, n = 6) is increased by ~3.73 ± 0.26 folds ($p < 0.0001$, ****) relative to controls (≈6.78%, n = 6). Likewise, the proportions of Nurr1+/Rorβ+ cells in EmxCre+ and NexCre+ mutant brains are elevated to similar levels ($p = 0.60$, ns): the proportion in EmxCre+ mutant brains (≈31.23%, n = 7) is increased by ~19.92 ± 0.72 folds ($p < 0.0001$, ****) relative to controls (≈1.49%, n = 7), and the proportion in NexCre+ cKO brains (≈30.59%, n = 7) is increased by ~19.02 ± 0.44 folds ($p < 0.0001$, ****) relative to controls (≈1.53%, n = 6). The statistics data was analyzed by two-tailed *Student's t*-test. Scale bar: 200 µm.

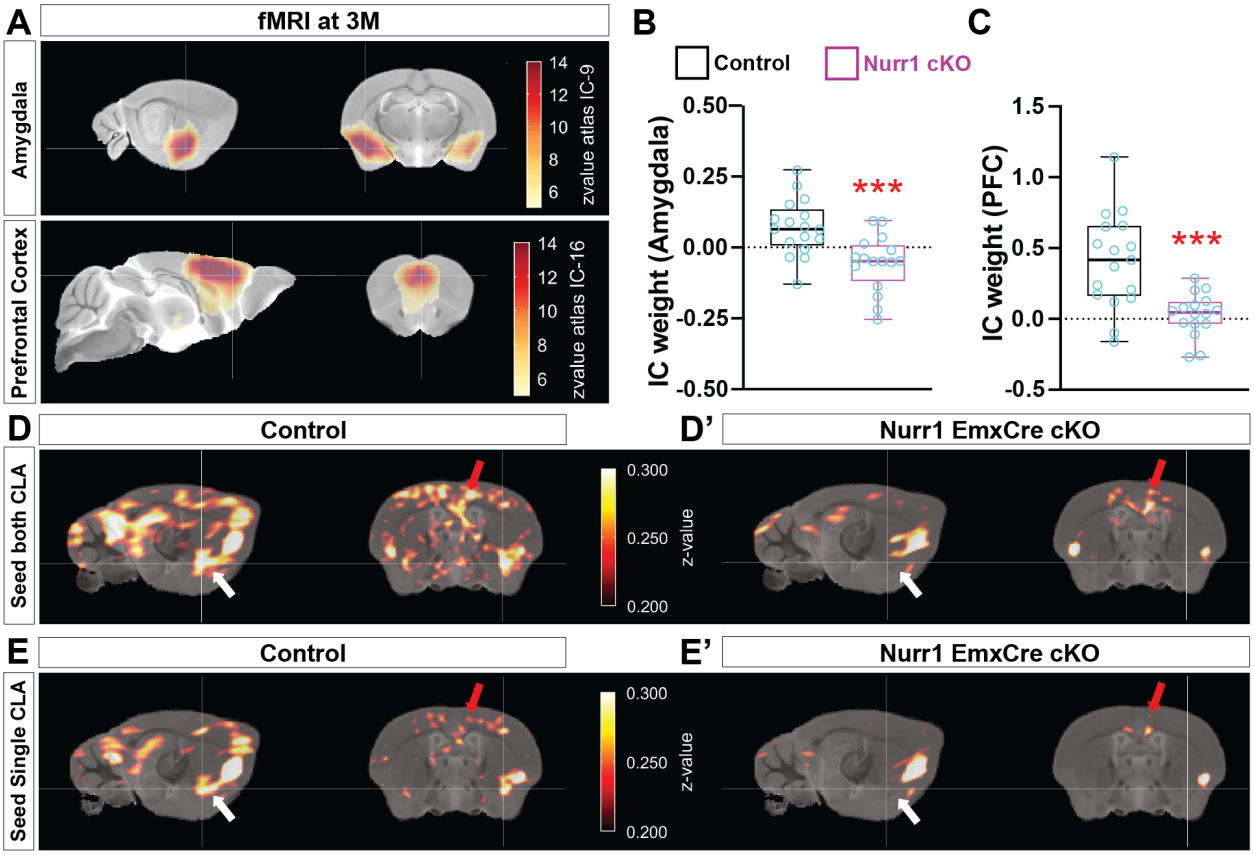

Figure 3 Connectivity networks associated with claustrum are impaired in Nurr1 deficient brains.

(A – C) Resting state fMRI (rs-fMRI) was used to examine functional connectivity of 17 networks of control and Nurr1 deficient brains. (**A**) Z-score analysis manifests the blood-oxygen-level dependent (BOLD) signal intensities in amygdala and prefrontal cortex (PFC) networks of control brains are positively over threshold values relative to those of mutant brains, suggesting these networks are impaired in Nurr1 deficient brains. (**B, C**) BOLD signals in rs-fMRI are represented as weighted average values measured by threshold free cluster enhancement (TFCE) approach derived from group IC analysis (see "*Materials and Methods*"). The IC weighted average value of amygdala network is ≈0.071 (n = 17) in control mice, but significantly reduced to ≈-0.056 (p = 0.00090, ***; n = 16) in Nurr1 deficient mice. The value of PFC network in control mice is ≈0.41 (n = 17), but reduced to ≈0.030 (by ~12.51 ± 3.04 folds, p = 0.00027, ***; n = 16) in Nurr1 deficient mice.

(D-D' and E-E') Seed-based connectivity mapping approach to analyze the connected networks to CLA. The synchronous BOLD signals of amygdala (white arrowheads) and PFC (red

arrowheads) networks in Nurr1 deficient brains are weakened in comparison to control brains when seeding either both (**D-D'**) or single (**E-E'**) hemispheric CLA as regions of interest.

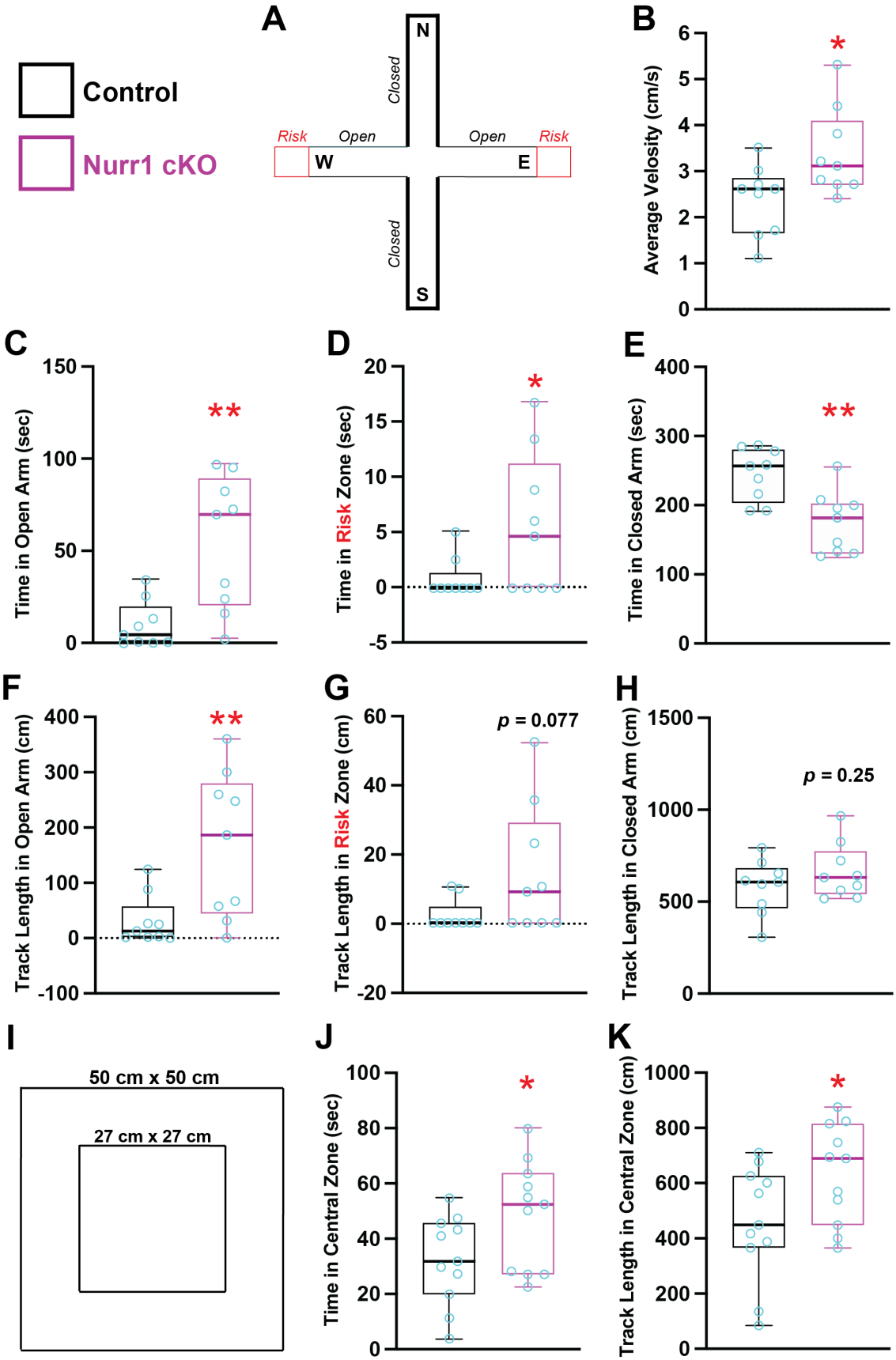
Control
Nurr1 cKO
A
N
S
W
E
Closed
Closed
Risk
Open
Open
Risk
B
Average Velosity (cm/s)
C
Time in Open Arm (sec)
D
Time in Risk Zone (sec)
E
Time in Closed Arm (sec)
F
Track Length in Open Arm (cm)
G
Track Length in Risk Zone (cm)
p = 0.077
H
Track Length in Closed Arm (cm)
p = 0.25
I
50 cm x 50 cm
27 cm x 27 cm
J
Time in Central Zone (sec)
K
Track Length in Central Zone (cm)

Figure 4 Nurr1 deficient mice are less susceptible when exposing to stressors.

(A – H) Analysis of mouse behaviors in elevated plus maze (EPM). (**A**) The apparatus used in EPM (also see "*Methods and Materials*"). The north (N) and south (S) arms are closed with barriers and west (W) and east (E) arms are open arms. The far-end ledge of open arms (10 cm) are defined as risk zones (red). (**B**) The velocity of Nurr1 deficient mice in EPM (≈3.38 cm/s, n = 9) was significantly higher than control mice (≈2.37 cm/s, n = 9), increased by ≈42.71% ± 17.10% (p = 0.024, *). **(C – E)** Nurr1 deficient mice spent more time in open arms (≈55.03 sec, n = 9) and risk zones (≈5.56 sec, n = 9) than control mice (open arms: ≈10.18 sec, n = 9; risk zones: ≈0.86 sec, n = 9), increased by ~4.41 ± 1.25 folds (p = 0.0028, **) and by ~5.49 ± 2.58 folds (p = 0.049, *), respectively, whereas Nurr1 deficient mice spent less time in closed arms (≈175.3 sec, n = 9) than control mice (≈244.9 sec, n = 9), decreased by ≈28.41% ± 7.91% (p = 0.0024, **). **(F – H)** Accordingly, Nurr1 deficient mice traveled longer distance in open arms (≈167.9 cm) and risk zones (≈14.48 cm) than control mice (open arms: ≈31.42 cm; risk zones: ≈2.28 cm), increased by ~4.34 ± 1.47 folds (p = 0.0095, **) and by ~5.36 ± 2.83 folds (p = 0.077, ns), respectively, but the track length of Nurr1 deficient mice (≈663.9 cm) is comparable to that of control mice (≈579.2 cm) in the closed arms (p = 0.25, ns).

(I – K) Analysis of mouse behaviors in open field (OF) test. (**I**) The schematic view of the open field test apparatus. (**J**) Nurr1 deficient mice spent more time in central zone of OF (≈48.67 sec, n = 11) than control mice (≈32.40 sec, n = 11), significantly increased by ≈ 50.22% ± 23.58% (p = 0.046, *). (**K**) The travel distance of Nurr1 deficient mice in the central zone (≈633.4 cm) is longer than that of control mice (≈456.3 cm), increased by ≈38.81% ± 18.12% (p = 0.045, *).

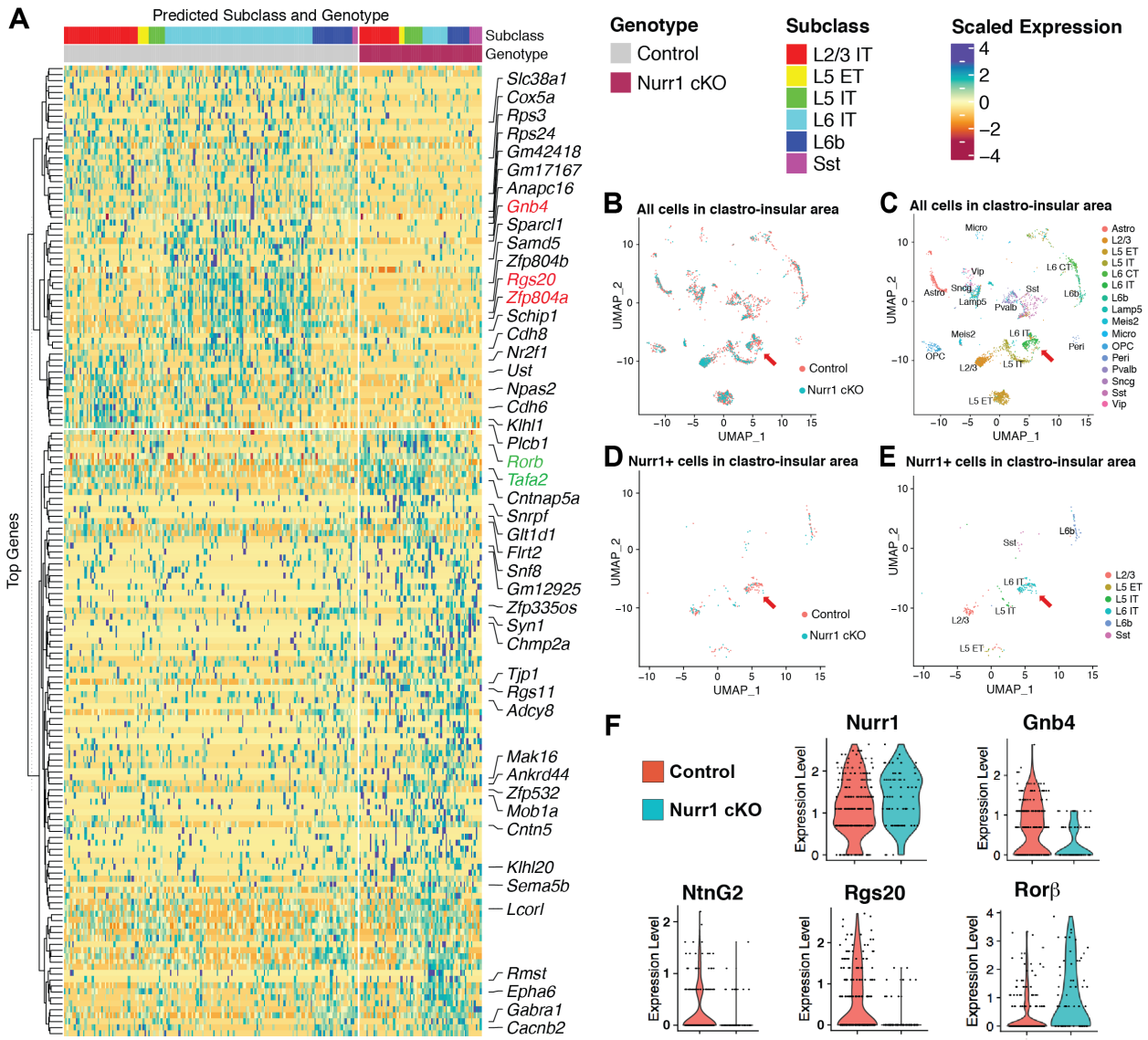

Figure 5 Single cell transcriptomic analysis of Nurr1+ cell populations in claustro-insular region at P0

(A) Heatmap of top-rated regulated genes by Nurr1. The map was generated based on single cell transcriptomics of claustro-insular cells in control (left panel) and Nurr1 deficient brains (right panel). Cell subclasses are marked by colors. The figure is separated by expression levels (downregulation: upper panel; upregulation: lower panel) and the expression scales are marked as deep red (-4) as minimal and dark blue (4) as maximal. Some key genes involved in the project are marked (downregulated in red and upregulated in green).

(B, C) Uniform manifold approximation and projection (UMAP) analysis of the single cell transcriptomes based on all cells isolated from claustro-insular tissues in control and Nurr1 deficient brains (**B**). Each point denotes an individual cell. Claustro-insular cell subclasses in

UMAP are grouped and marked by colors in (**C**). Nurr1+ CLA cell population is pointed by a red arrowhead (L6 cluster in Azimuth annotation[39], the same as **D, E**). Astro, astrocytes; L2/3, layer 2 and 3 cells; L5 ET and IT, layer 5 extra- and intra-telencephalon projecting glutamatergic neurons; L6 CT and IT, layer 6 corticothalamic and intratelencephalon projecting glutamatergic neurons; L6b, layer 6b neurons (Sp); Micro, microglia; OPC, oligodendrocyte precursor cells; Peri, pericytes; GABAergic neuron clusters: Lamp5, Meis2, Pvalb, Sncg, Sst, Vip.

(D, E) UMAP analysis of Nurr1+ cell populations in claustro-insular region of control and Nurr1 deficient brains. Nurr1+ cell subclasses are marked by colors in (**E**), which are mainly distributed in L2/3, L6 IT and L6b of cortex, consistent with Nurr1 expression pattern.

(F) Violin plots for selected genes expressed in CLA. The levels of Nurr1-Cterm transcripts in claustro-insular cells of control and Nurr1 deficient brains are equivalent. However, expression levels of Gnb4, NtnG2 and Rgs20 are downregulated in claustro-insular region of Nurr1 deficient brains, whereas the expression level of Rorβ is upregulated.

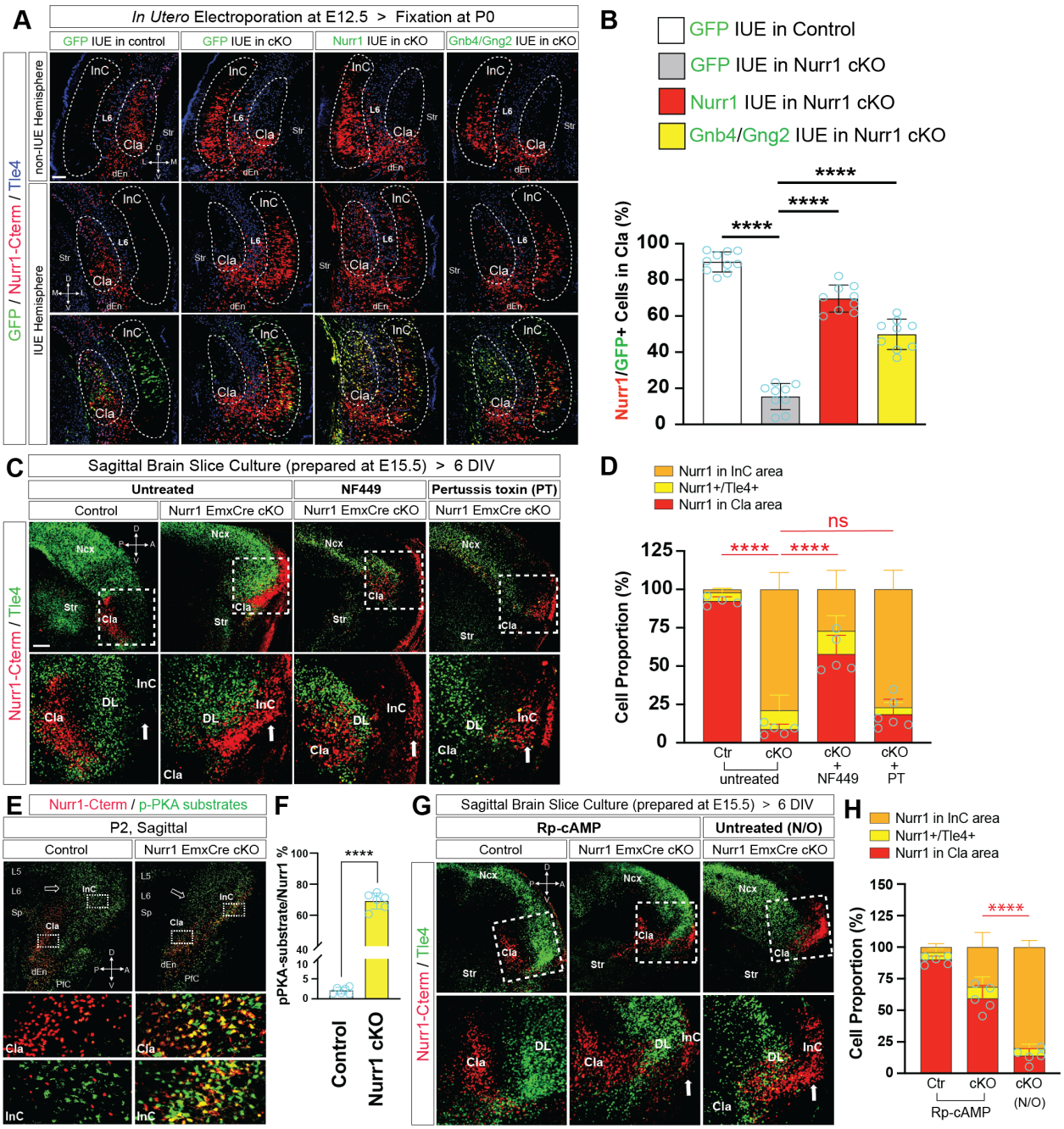

Figure 6 Nurr1 regulates claustral neuron positioning by suppressing Gαs-PKA signaling.

(A, B) IF for Nurr1-Cterm (red) and Tle4 (blue) on the coronal sections of non-electroporated (non-IUE) and electroporated hemispheres of control and EmxCre mutant brains at P0 (**A**) and quantification for the proportions of Nurr1-Cterm+/GFP+ cells resident in CLA relative to all double positive cells in various electroporation conditions (**B**). The non-electroporated hemispheres serve as comparison references to the electroporated ones of the same brains. IUE of GFP into embryos at E12.5 demonstrates almost all double positive cells reside in normal CLA of

control brains (≈89.94%, n = 10), but IUE of GFP into Nurr1 deficient embryos reduces the proportion to ≈15.44% (n = 9), depicting Nurr1 deficient cells largely migrate across Tle4+ L6 cells and disperse in InC. Nurr1-GFP bicistronic electroporation into mutant embryos restricts the Nurr1-Cterm+ cells in the CLA area, elevating the proportion by ~3.51 ± 0.22 folds (≈69.63% ± 3.47%, $p < 0.0001$, ****; n = 9) relative to that of GFP IUE into mutant embryos. Moreover, Gnb4/Gng2 co-electroporation into mutant embryos restricts a subpopulation of Nurr1-Cterm+ cells in the CLA area, elevating the proportion by ~2.23 ± 0.24 folds (≈49.89% ± 3.70%, $p < 0.0001$, ****; n = 9) relative to that of GFP IUE into mutant embryos. Notably, the Nurr1-Cterm+ cells in the Nurr1- or Gnb4/Gng2-electroporated mutant hemispheres are visibly less in InC areas than their non-electroporated contralateral hemispheres. The statistical data are analyzed by two-tailed *Student's t*-test (the same below). Scale bar: 100 μm.

(C, D) IF for Nurr1-Cterm (red) and Tle4 (green) on the sagittal brain slices of control and EmxCre mutant brains (**C**) and quantification for the proportions of Nurr1-Cterm+ cells resident in CLA (red bars) relative to all Nurr1-expressing cells (**D**). The brain slices were prepared at E15.5 and cultured for 6 days *in vitro* (DIV). The Nurr1+ CLA neurons (≈92.29%, n=4) are properly positioned in control brains, but only a small fraction of Nurr1-Cterm+ cells (≈8.78%, n=5) can be detected posterior to Tle4+ DL neurons in Nurr1 deficient slices. (**D**) The proportion of Nurr1-Cterm+ cells in CLA of mutant brains is increased by ~5.58 ± 0.65 folds when NF449 (10 μm) was applied (≈57.74% ± 5.72%, $p < 0.0001$, ****; n = 5), but not significantly altered when pertussis toxin (PT, 100 ng/ml) was applied (≈18.65% ± 4.62%, $p = 0.062$, ns; n = 6), relative to that of untreated mutant brains. White arrowheads in (**C**) and (**G**) indicate the Nurr1-expressing cells in InC. Scale bar: 200 μm.

(E, F) IF for Nurr1-Cterm (red) and phosphorylated PKA substrates (green) on the sagittal sections of control and EmxCre mutant brains at P2 (**E**) and quantification for the proportions of double positive cells relative to all Nurr1-expressing cells (**F**). The Nurr1-Cterm+ cells in Nurr1 deficient brains exhibit tremendously elevated levels of PKA substrate phosphorylation (≈69.07% ± 2.14%, n = 6) compared with that of control brains (≈2.06%, n = 6).

(G, H) IF for Nurr1-Cterm and Tle4 on the sagittal brain slices and quantification for the proportions of Nurr1-expressing cells in CLA as in (**C, D**). Rp-cAMP (100 μm) treated Nurr1+ cells in control brains are mostly located in CLA (≈90.05%, n=5), and seem normal as that of untreated control brains (≈92.29%, **D**). The proportion of Nurr1-Cterm+ cells in the CLA of Rp-

cAMP treated mutant hemispheres is increased up to ≈59.30% ± 5.28% ($p < 0.0001$, ****; $n = 5$) in comparison to that of untreated mutant hemispheres (≈13.96%, $n = 5$).